

Accretion Induced Collapse and Electron Capture Supernovae

Seminar talk by Stephan Wawoczny, TUM, advised by Dr. Ashley J. Ruiter, MPA

Outline:

- **White Dwarfs in general**
- **Accretion induced collapse**
- **Electron capture supernovae**
- **Conclusion**

White Dwarfs in general

- Nuclear composition depends on mass of progenitor star, most abundant are WDs consisting of C/O. Also possible: WDs consisting of O/Ne/Mg
- Stabilised by degenerate electron gas pressure, given by:

$$P_e = \frac{\pi^3}{15m_e} \hbar^2 \left(\frac{3n_e}{\pi} \right)^{5/3} \quad n_e = \frac{N_e}{V}$$

→ White Dwarfs can be described with the **Polytrope Model**:

$$P = K\rho^{1+\frac{1}{n}}$$

with the density function given by $\rho = \rho_c \phi^n$, the Lane-Emden Equation:

$$\frac{1}{r^2} \frac{d}{dr} \left[\frac{r^2}{\rho} \frac{dP}{dr} \right] = -4\pi G \rho r^2$$

and setting: $r = \left(\sqrt{\frac{K(n+1)}{4\pi G \rho_c^{1-\frac{1}{n}}}} \right) \xi$, we get the following equation

$$\frac{1}{\xi^2} \frac{d}{d\xi} \left[\xi^2 \frac{d\phi}{d\xi} \right] = -\phi^n$$

This leads to the following mass formula:

$$M = -4\pi\rho_c \left(\frac{K(n+1)}{4\pi G \rho_c^{1-\frac{1}{n}}} \right)^{\frac{3}{2}} \left(\xi^2 \frac{d\phi}{d\xi} \right)_{\xi^*}$$

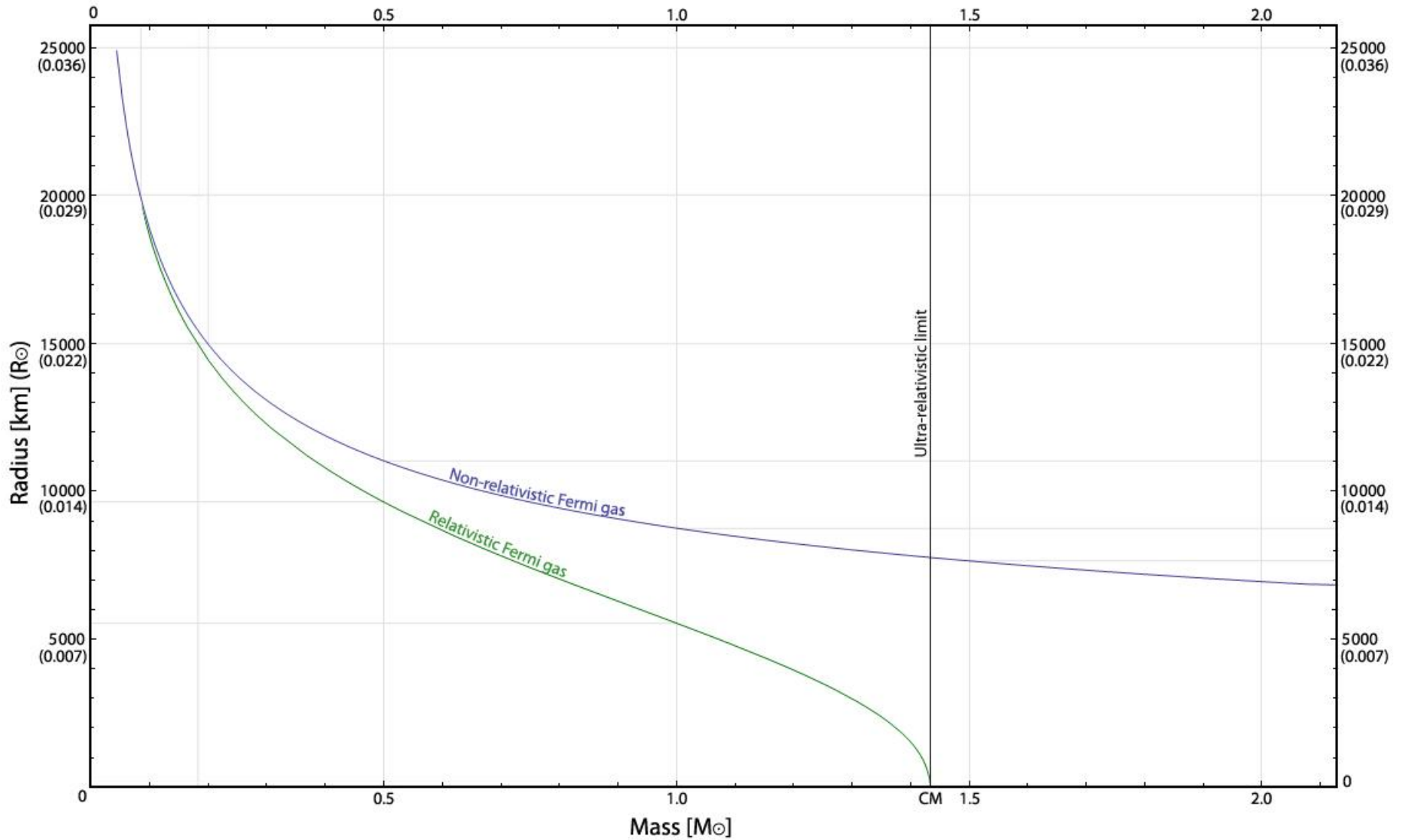
For WD, stabilised by degenerate electron gas: $n = 1.5$

Assuming relativistic degenerate electron gas, pressure is given by:

$$P_e^{rel} = \frac{\hbar c \pi^{\frac{2}{3}}}{12} (3\rho N_A Y_e)^{\frac{4}{3}}$$

Therefore $n = 3$ and: $M = -36\pi^2 \left(\frac{\hbar c}{12\pi G} \right)^{\frac{3}{2}} (N_A Y_e)^2 \left(\xi^2 \frac{d\phi}{d\xi} \right)_{\xi^*} \approx 5.81 \cdot Y_e^2 M_{\odot}$

That's Chandrasekhar's mass limit for WDs



http://upload.wikimedia.org/wikipedia/commons/8/81/WhiteDwarf_mass-radius.jpg

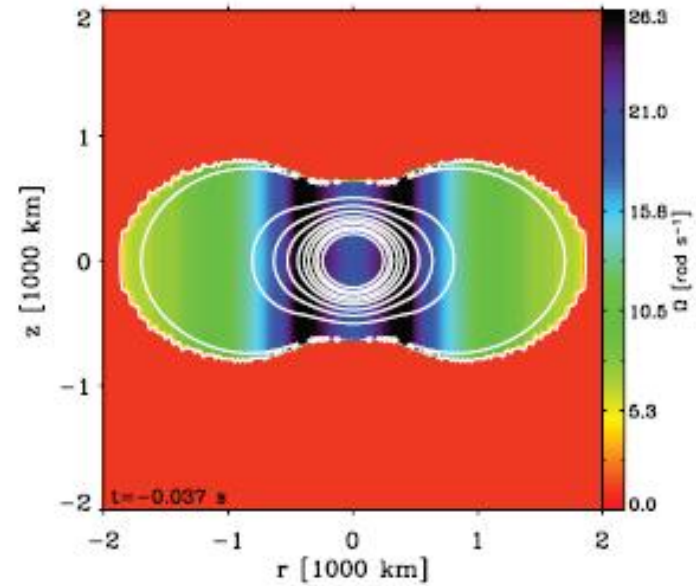
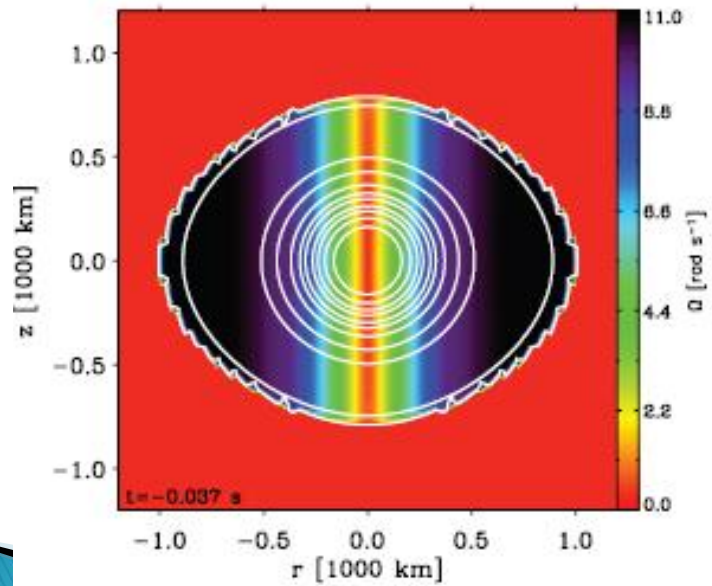
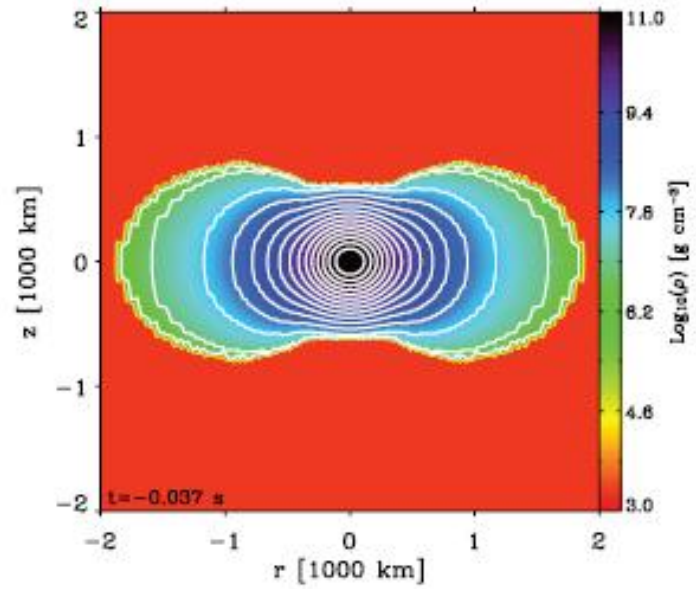
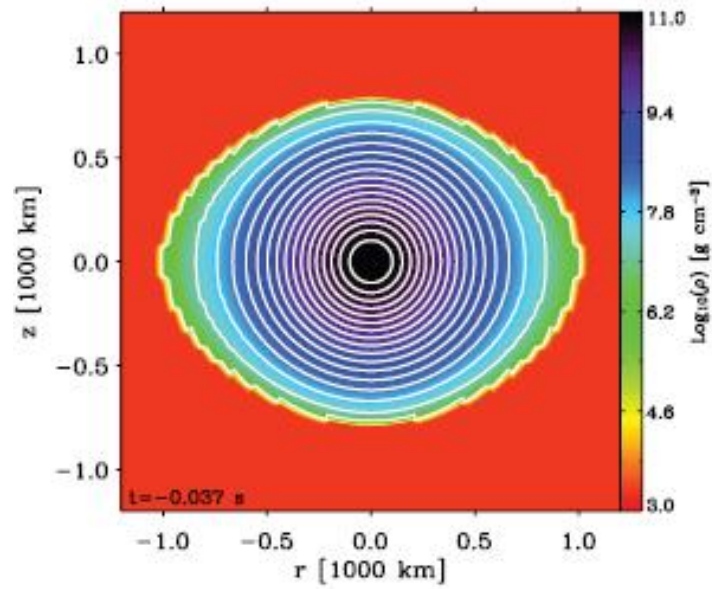
Accretion – Induced Collapse

- O/Mg/Ne White Dwarfs undergo accretion induced collapse, if they exceed Chandrasekhar-mass by accreting matter from a binary companion
- Due to accretion of matter → Gain of angular momentum
→ Centrifugal force compensates gravitational force partially
- M_{Ch} larger than for not-rotating WDs

TABLE 1
PROPERTIES OF SELECTED AIC PROGENITORS

M (M_{\odot})	R_p (km)	R_{eq} (km)	J (ergs s) ($\times 10^{50}$)	T (ergs) ($\times 10^{50}$)	$ W $ (ergs) ($\times 10^{50}$)	$T/ W $	
						Initial	Final
1.46.....	800	1130	0.160	0.7	91.97	0.0076	0.059
1.92.....	660	2350	1.092	10.57	126.9	0.0833	0.262

Dessart et al., 2006, ApJ, 644, 1063



Dessart et al., 2006, ApJ, 644, 1063

At $M_{WD} = M_{Ch}$ the electrons become relativistic because: $E_F = m_e c^2$

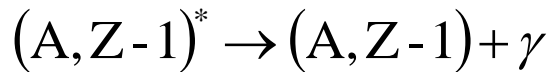
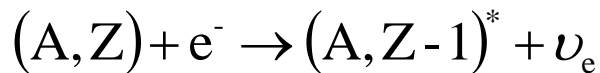
→ relativistic degenerate electron gas pressure too small to stabilise WD

→ WD collapses quasi-dynamically

→ Fermi energy of the electrons rises as:

$$E_F \approx \hbar c n_e^{1/3}$$

→ Fermi energy larger than E_{thr} for Electron Capture Reactions on ^{24}Mg and ^{24}Na



$$E_{thr} \equiv E_{thr,0} + E_{\gamma,0}$$

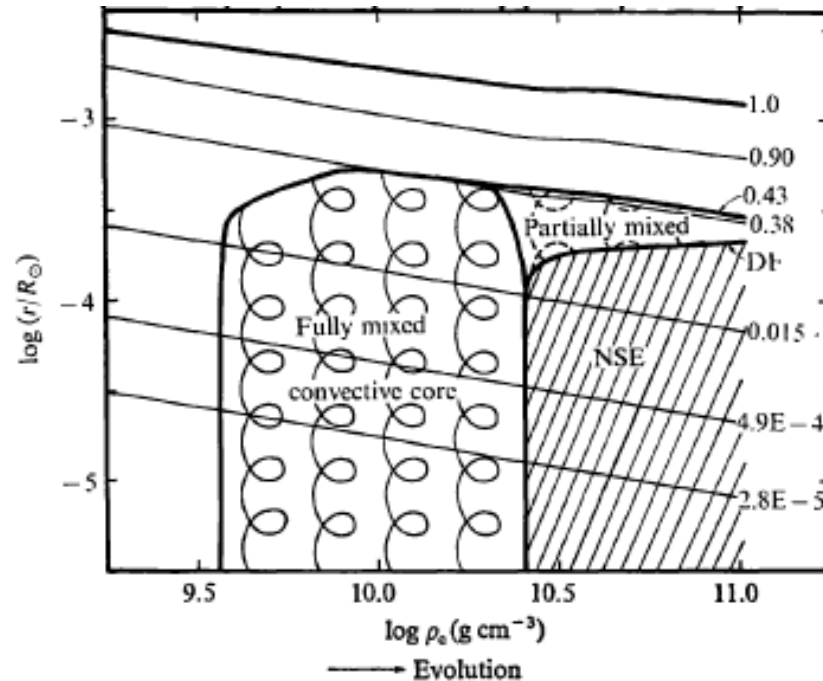


Fig. 1. Contraction of shells with constant mass fractions $q = M_r/M_{\text{core}}$ are shown against the central density. Attached numbers are their mass fractions. Convective core, NSE core, and deflagration front (DF) are also shown. The edge of the convective core in its farthest extension corresponds to the shell with $q=0.43$.

Miyaji et al., 1980, PASJ, 32, 303

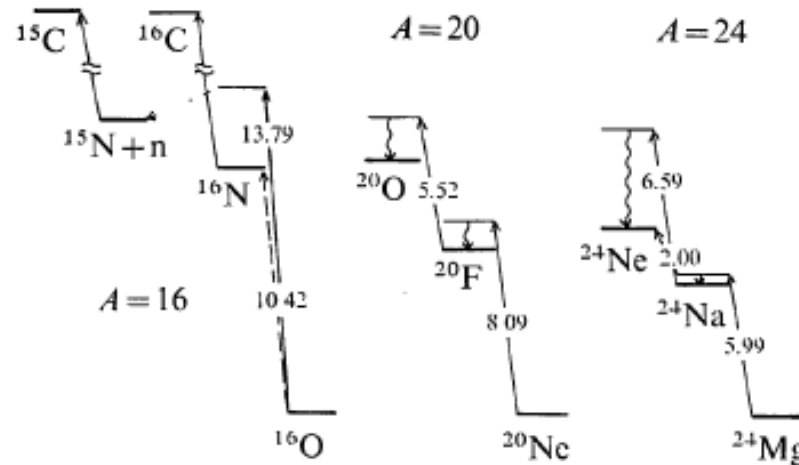


Fig. 2. Schematic energy diagrams of allowed transitions of electron captures with the lowest energy differences, which are given in table 2. For the case of ^{16}O , the unique first forbidden transition is shown by the dashed arrow and neutron emission (drip) from its daughter nucleus ^{16}N is shown by the dotted arrow. Energy differences are given in units of MeV.

Table 2. Threshold energies and densities for electron captures.

Parent nucleus	$E_{\text{thr},0}$ (MeV)	E_{thr} (MeV)	$\log \rho_{\text{thr}}(Y_e/0.5)$ (g cm^{-3})
^{24}Mg	5.52	5.99	9.60
^{24}Na (ground)	2.47	6.59	9.72
^{24}Na (isomer)		2.00	8.33
^{20}Ne	7.03	8.09	9.96
^{20}F	3.82	5.52	9.50
^{16}O	10.42	10.42	10.28

- Entropy production by electron captures leads to formation of a convective core
- With rising E_F due to collapse, other nuclei start to capture electrons. The β -decay of daughter nuclei is not possible or very slow because of high E_F
- Oxygen deflagration becomes dominant process at a central density of $\rho_c = 2.5 \cdot 10^{10} \text{ g} \cdot \text{cm}^{-3}$

- No detonation because of small nuclear energy release of only 0.4 MeV compared to $E_F = 10$ MeV
- Deflagration front stays at constant Radius $r_{DF} \cong 10^{-4} R_\odot$ and is propagating outwards in phase only. Each shell ignites oxygen deflagration when it reaches the critical density (s.a.)

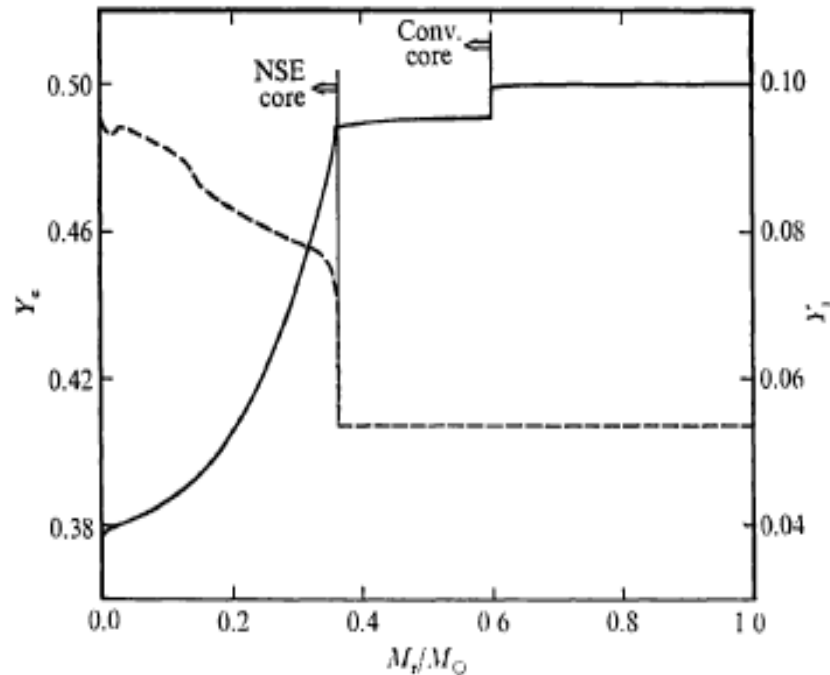
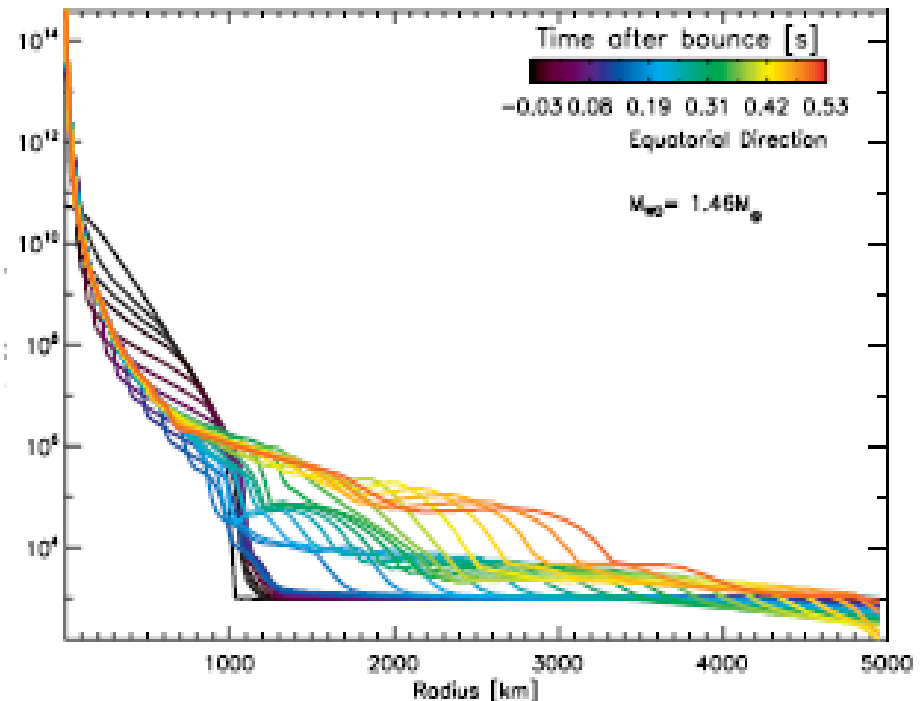
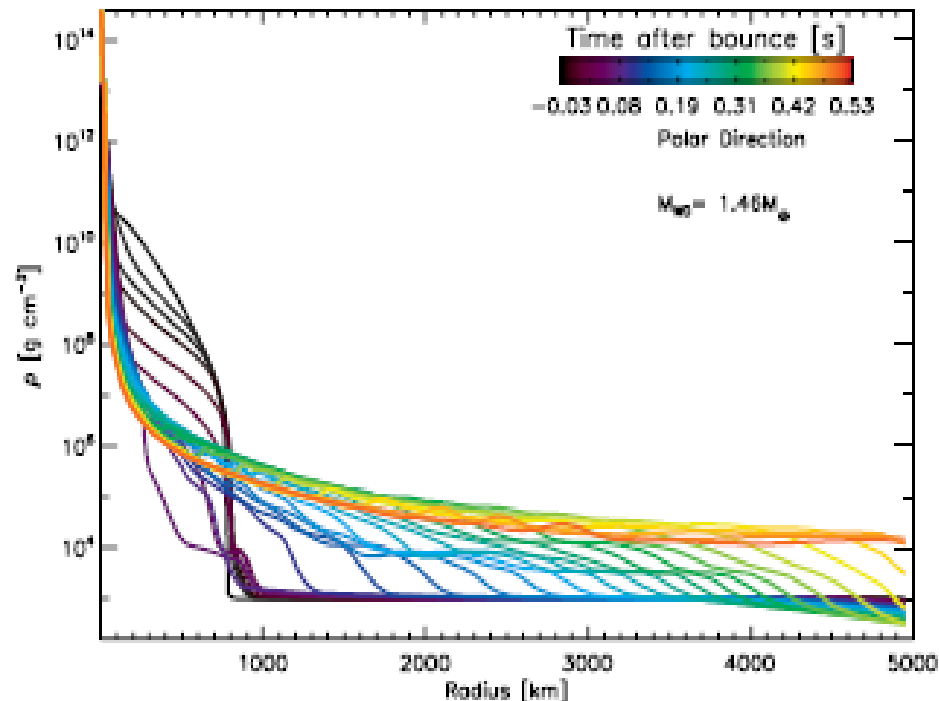


Fig. 13. Distribution of mole numbers for electrons (solid curve) and for ions (dashed curve) through the core for the stage #8. Beyond $M_r \cong 0.7 M_\odot$, they are constant up to the core edge.

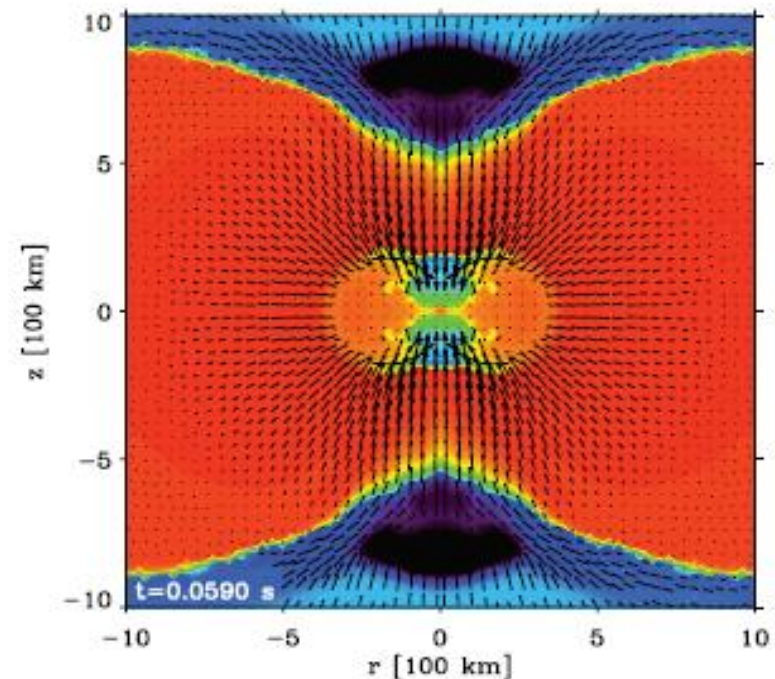
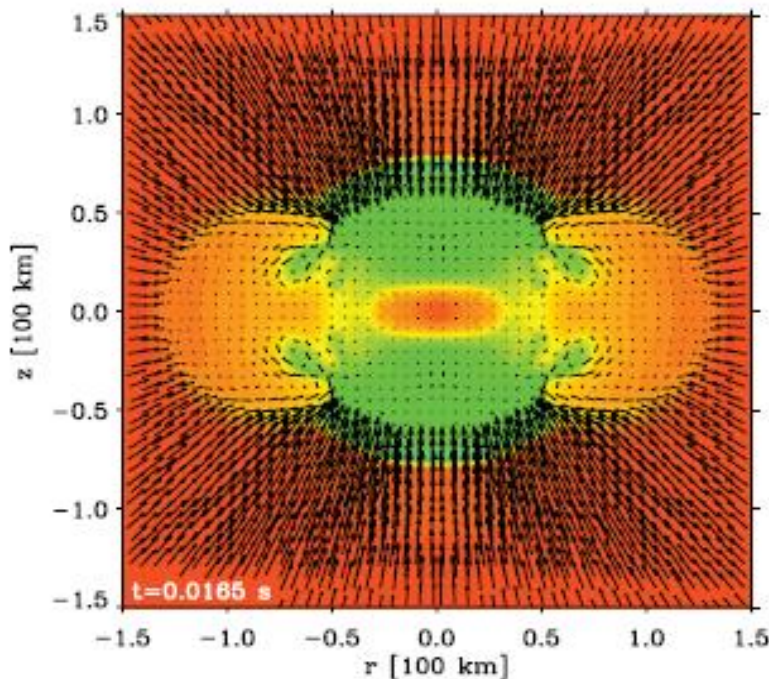
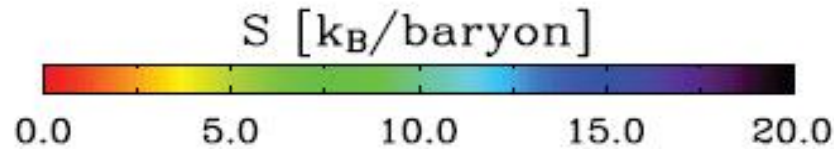
Miyaji et al., 1980, PASJ, 32, 303

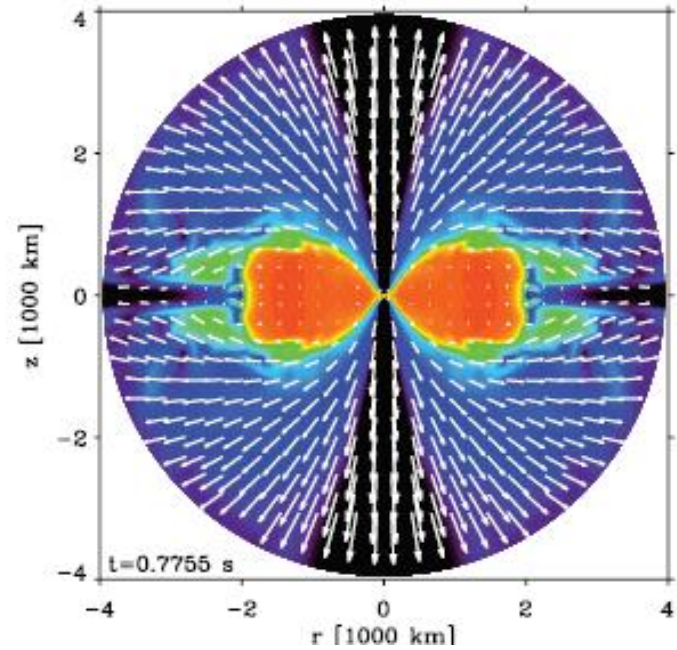
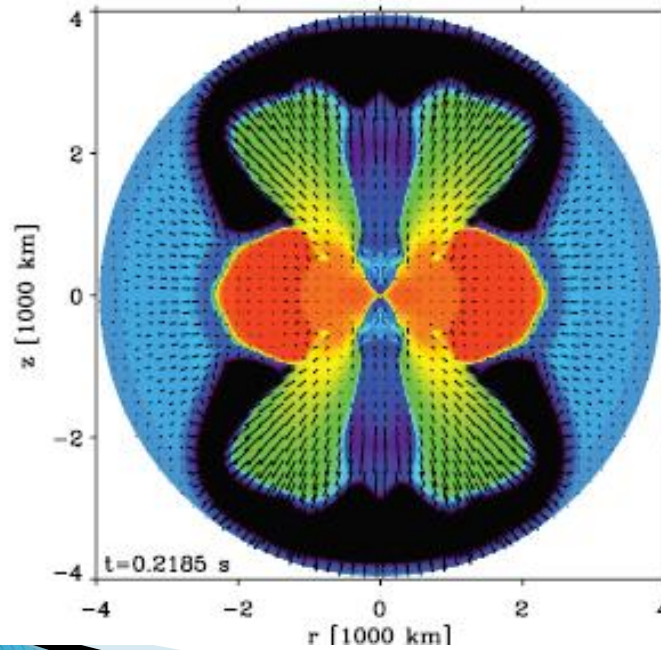
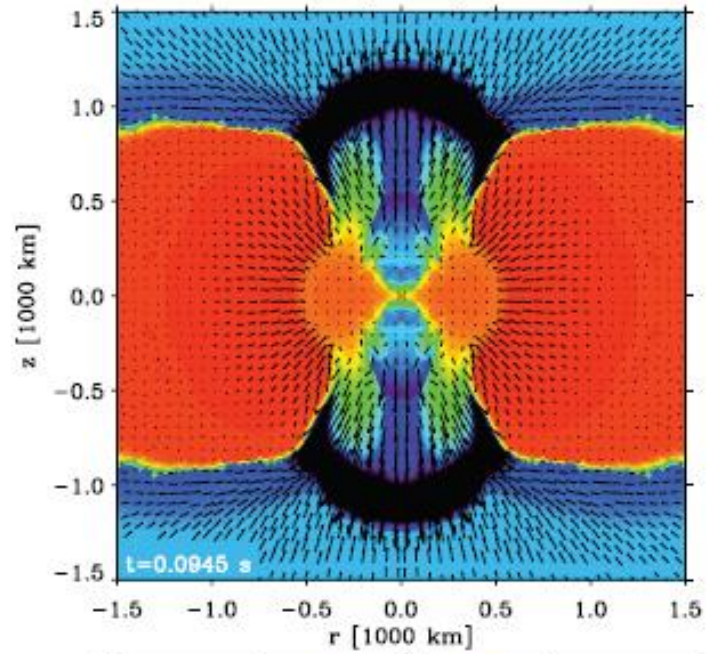
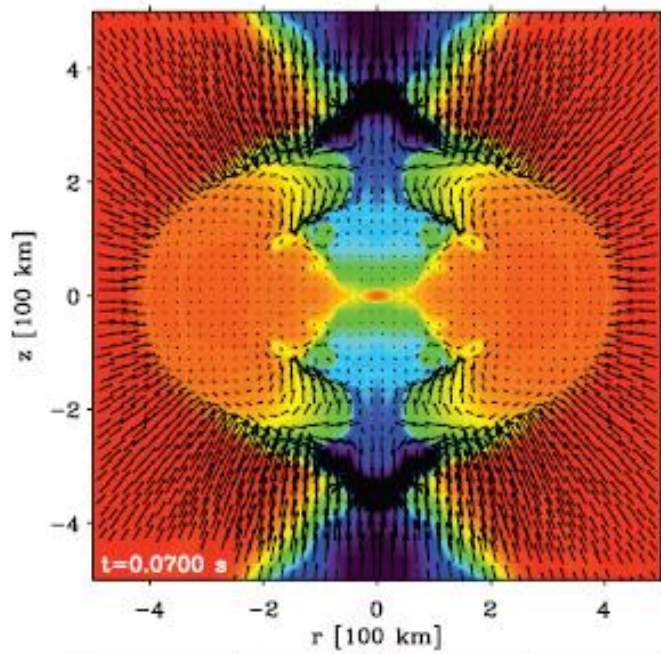
- Through the deflagration front the material is processed into NSE
- Due to high pressure most of the EC happen in the NSE core → Y_e decreases
- Due to decreasing Y_e , M_{Ch} decreases → collapse accelerates
- As the collapse continues EC produces nuclei at neutron drip line → free neutrons are produced
- At densities near nuclear density neutrinos are trapped in the core



Dessart et al., 2006, ApJ, 644, 1063

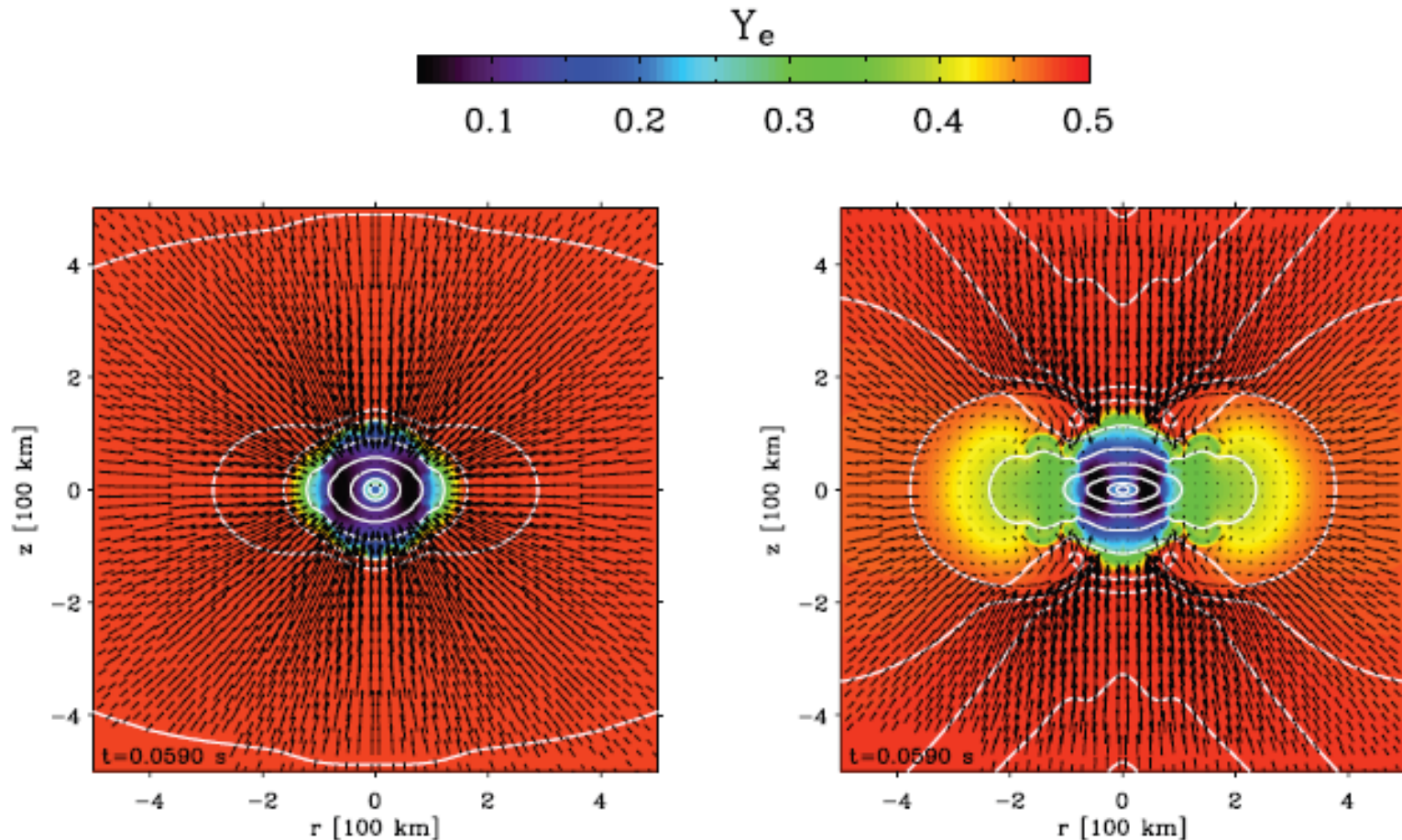
- Collapse stops at a density higher than nuclear density \rightarrow shockwave moving outwards without stalling. Outer layers not yet started to fall in.
- Progress of the shock at low latitudes supported by centrifugal force
- No stalling in polar direction because of steeper density gradient. Shock reaches surface earlier than at low latitudes. Sweeps up the ambient medium at an opening angle determined by the remnant disk \rightarrow wraps around disk

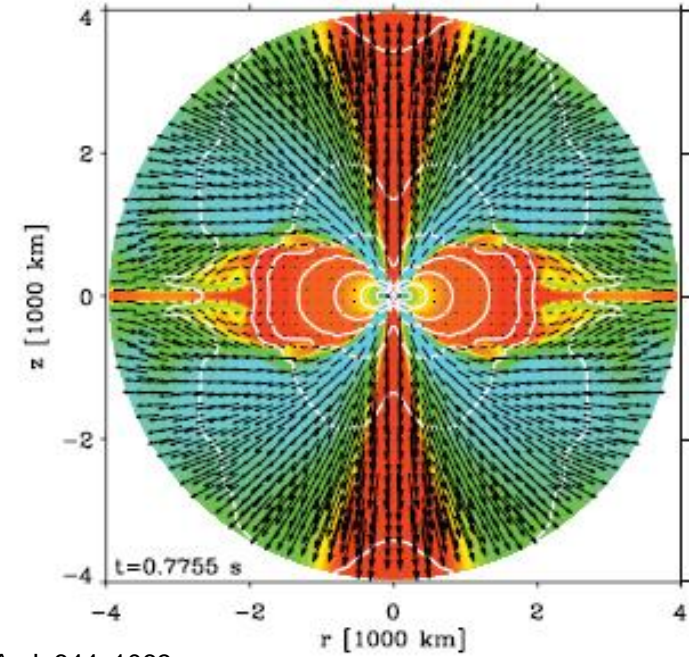
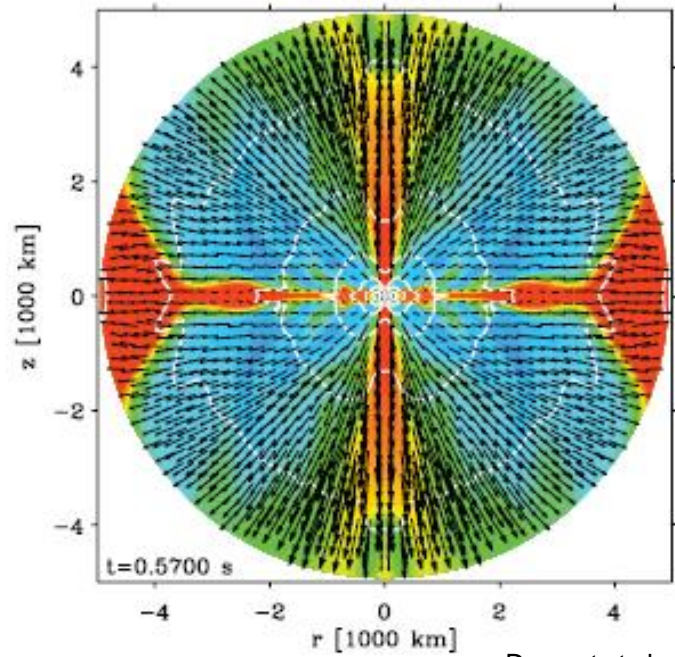
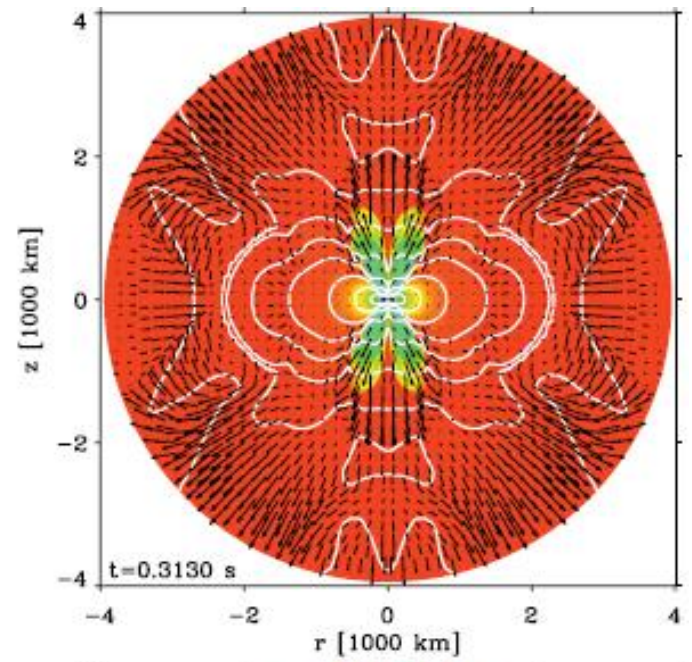
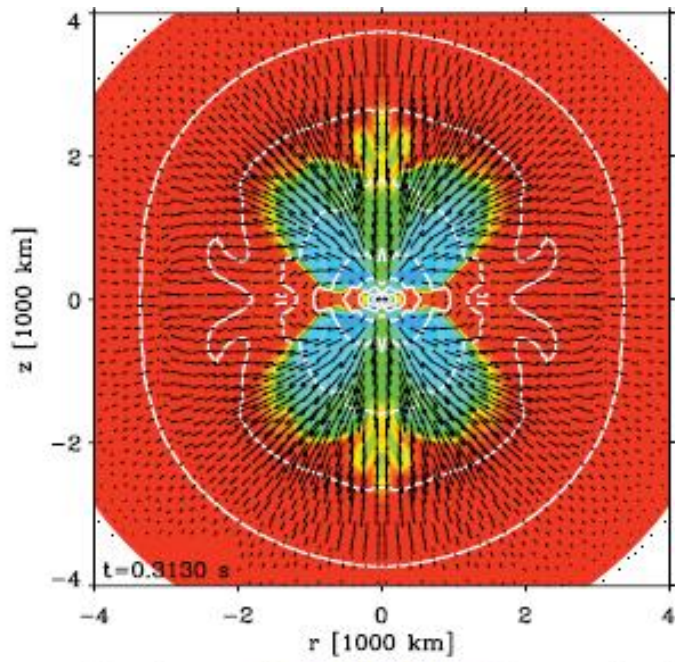




Dessart et al., 2006, ApJ, 644, 1063

- Strong neutrino driven wind sets in, consisting of dense, low Y_e material, in contrast to material ejected in the blast
- The neutrino driven wind is very angle-dependent, around 30000 km s^{-1} at the pole and 30% less at 40°

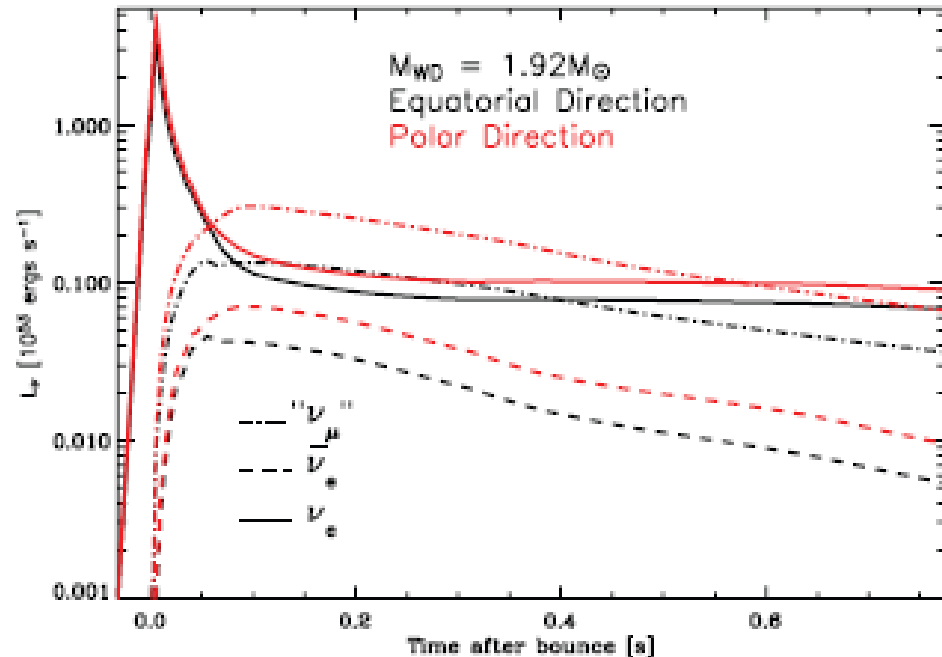
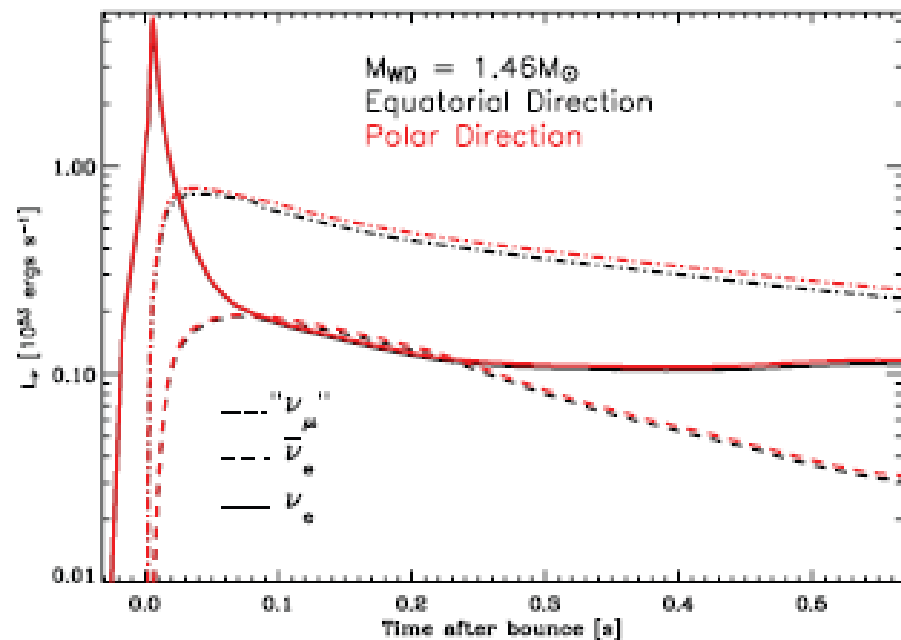




Dessart et al., 2006, ApJ, 644, 1063

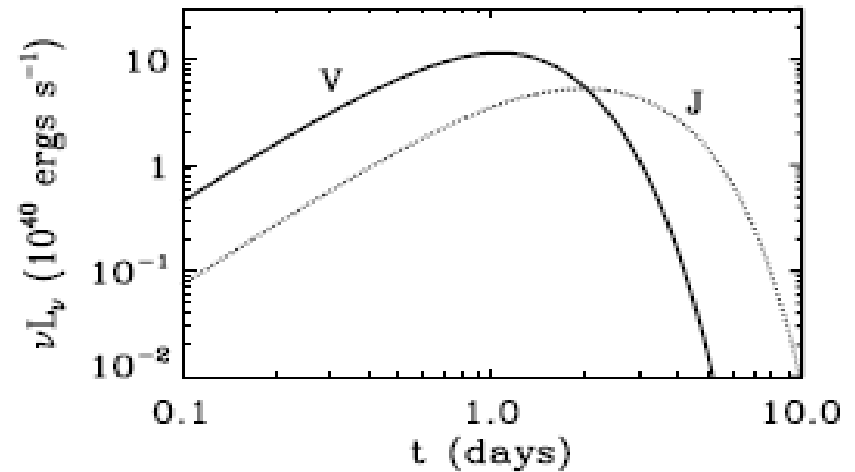
Observational Signatures

- Shortly after bounce: high neutrino luminosity, similar to core collapse SN. With a maximum of $L_\nu = 5.2 \cdot 10^{53} \text{ ergs} \cdot \text{s}^{-1}$
- Most luminosity by ν_e , but also contribution by thermally produced ν of other flavours \rightarrow less ν in heavier WD model because of weaker bounce and lower temperatures



Dessart et al., 2006, ApJ, 644, 1063

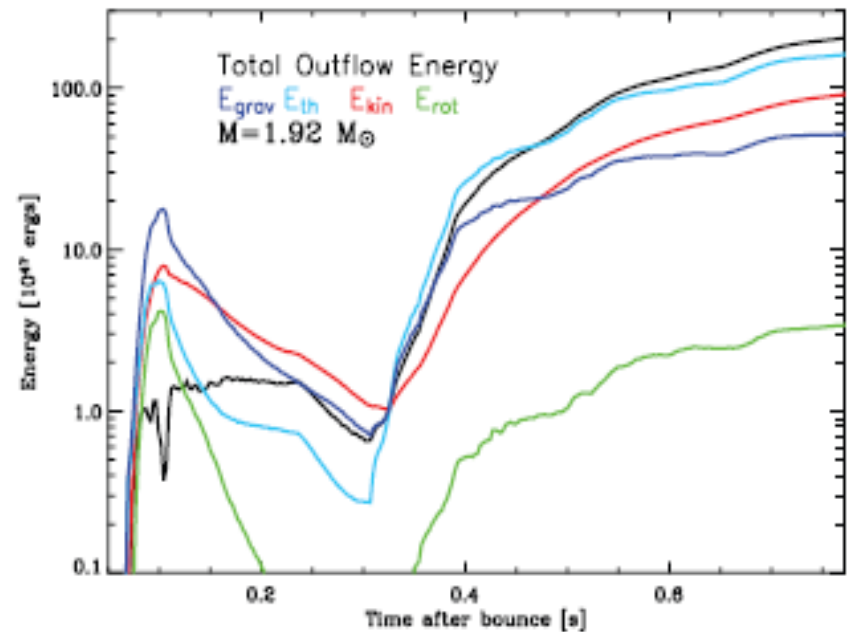
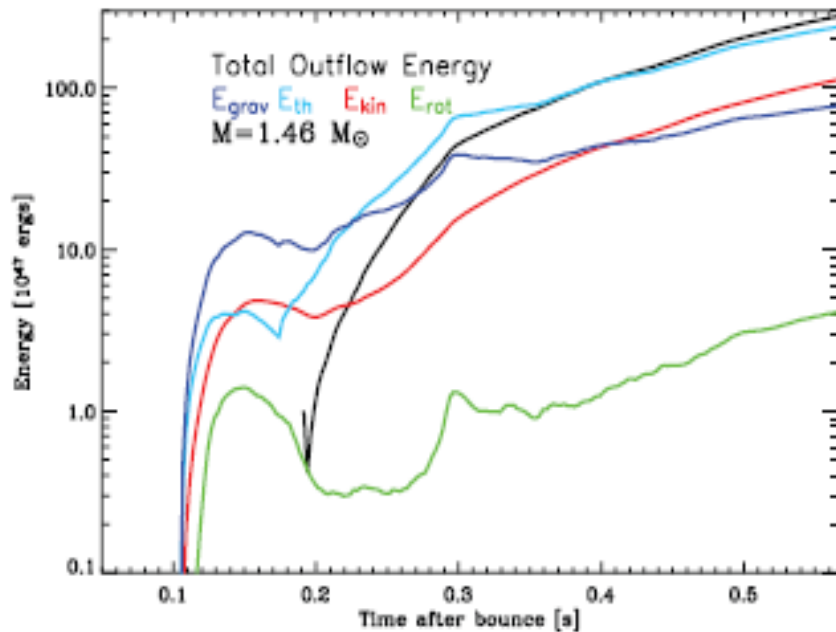
- Luminosity peaks around one day after bounce
- Total ejected Mass and ejected Ni mass in order of $10^{-2} M_{\odot}$
- Few intermediate mass elements synthesized \rightarrow spectroscopically distinct from other SN



Metzger et al., 2009, MNRAS, 396, 1659

- Galactic rate predicted by binary population synthesis models to be in the range $R_{AIC} \sim 10^{-6} - 10^{-4} \text{ yr}^{-1}$; to match nuclear abundances in the solar system $R_{AIC} \leq 10^{-4} \text{ yr}^{-1}$

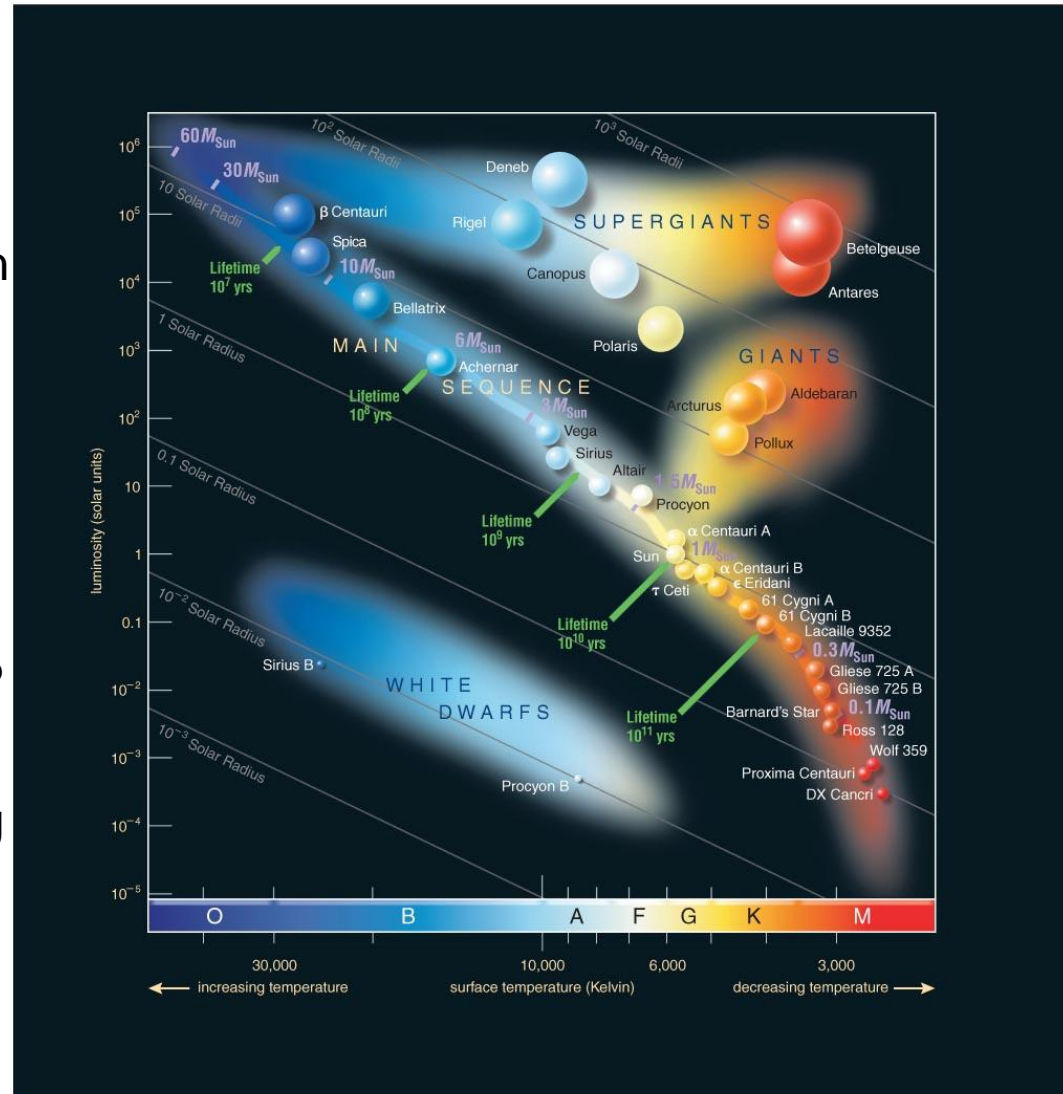
- Total emitted energy between $5 \cdot 10^{49}$ to 10^{50} ergs
- About one order of magnitude smaller than core collapse SN, because of too little mass being able to absorb neutrinos
- Bumps caused by episodic mass loading of the neutrino driven wind



Dessart et al., 2006, ApJ, 644, 1063

Electron Capture Supernovae

- Stars of masses in the range of 8-12 M_{\odot} end their lives with supernovae triggered by EC
- Massive enough to burn carbon in the core under non-degenerate conditions
- After exhaustion of carbon in the core, a degenerate core consisting of O/Ne/Mg appears interior to a helium core of 2-3 M_{\odot}
- Growth of the core at first controlled by carbon shell burning until its mass exceeds 1.2 M_{\odot} then by helium shell burning



Copyright © 2008 Pearson Education, Inc., publishing as Pearson Addison-Wesley.

- Neon burning does not ignite because the maximum attained temperature is too low
- The core is cooled by neutrino losses and heated by the burning shells outside → core cooler than shell
- Very slow growth of the core by hydrogen burning after mixing of helium zone and hydrogen rich envelope due to convection → further cooling by neutrinos
- As the core reaches M_{Ch} it starts to collapse and EC start. Further development similar to that of a WD in AIC
- Shockwave generated by core bounce will blow away hydrogen and probably helium envelope → no further accretion on NS and collapse to black hole

Conclusion

- O/Ne/Mg WD accretes to M_{Ch} → collapse → EC reactions start → NS as remnant
- $10^{-2} M_{\odot}$ of material ejected from accretion disk, mainly ^{56}Ni
- Under energetic and sub luminous explosions
- Rare event because of low abundance of O/Ne/Mg WD especially in binary systems
- Not yet verified through observations, but possible explanation for sub luminous SN like SN2008ha and SN2008S

References:

- Shapiro, Teukolsky, “Black Holes, White Dwarfs and Neutron Stars; The Physics of Compact Objects”, 1983, Wiley-Interscience
- <http://spacefellowship.com/news/art15308/theoretical-supernova-actually-exists.html>
- Dessart et al., 2006, ApJ, 644, 1063
- Metzger et al., 2009, MNRAS, 396, 1659
- Miyaji et al., 1980, PASJ, 32, 303
- <http://www.physast.uga.edu/~jss/1020/ch15/16-10.jpg>
- Wanajo et al., 2009, ApJ, 695, 208
- Poelarends et al., 2008, ApJ, 675, 614
- Thielemann et al, 2005, Nuclear Physics A, 751, 301c-326c
- Nomoto et al., 1984, ApJ, 277, 791
- Woosley et al., 1994, ApJ, 433, 229
- http://upload.wikimedia.org/wikipedia/commons/8/81/WhiteDwarf_mass-radius.jpg